NANO LETTERS

2006
Vol. 6, No. 6
1297−1302

V_2O_5 Nanorods on TiO_2 Nanofibers: A New Class of Hierarchical Nanostructures Enabled by Electrospinning and Calcination

Rainer Ostermann,[†] Dan Li,[†] Yadong Yin,[‡] Jesse T. McCann,[†] and Younan Xia*[,†]

Department of Chemistry, University of Washington, Seattle, Washington 98195-1700, and The Molecular Foundry, Lawrence Berkeley National Laboratory, Berkeley, California 94920

Received April 25, 2006

ABSTRACT

Electrospinning provides a simple approach to fabricating nanofibers and assemblies with controllable hierarchical structures. In this communication, we demonstrate that electrospinning can be combined with calcination to further maneuver the morphology and phase structure of nanofibers. More specifically, single-crystal V_2O_5 nanorods could be grown on rutile nanofibers by carefully calcining composite nanofibers consisting of amorphous V_2O_5, amorphous TiO_2, and poly(vinylpyrrolidone). The size of the resulting V_2O_5 nanorods could be conveniently controlled by varying the composition of the nanofibers and/or the calcination temperature. In addition to the nanorod-on-nanofiber hierarchical structure, we believe this approach can also be extended to fabricate other more complex architectures.

Synthesis of hierarchical nanostructures with controllable sizes, shapes, and compositions has received increasing attention in recent years.[1] Such complex architectures, especially those based on one-dimensional nanostructures, are expected to display novel functions important to the development of advanced devices and systems. Notable examples include the synthesis of hierarchically structured nanowires (e.g., nanowire-on-nanowire) including ZnO/In_2O_3,[1d] SnO,[1e] ZnO,[1f] SnO_2-doped In_2O_3,[1g] and GaP/Ga(As)-P[1h] by controlled, stepwise growth via a vapor−liquid−solid growth process and the preparation of SnO_2/Fe_2O_3 by hydrothermal synthesis.[1i] We have recently demonstrated that metal nanoparticles with different shapes could be deposited on electrospun titania nanofibers by postspinning photocatalytic reduction to generate metal/oxide hierarchical assemblies.[2] In this communication, we demonstrate that V_2O_5 nanorods could grow directly from electrospun nanofibers composed of amorphous TiO_2/V_2O_5 to generate nanorod-on-nanofiber hierarchical structures during calcination. We noticed that Hou and Reneker have demonstrated that carbon nanotubes could grow on electrospun carbon fibers to form nanotube-on-nanofiber structures by incorporating iron catalysts in the fibers, followed by iron-catalyzed growth of carbon nanotubes using hexane vapor as the carbon source.[3] No additional source of V_2O_5 is required in the present work as all components are included in the nanofibers during the electrospinning process. Taken together, these studies clearly demonstrated that nanostructures more complex than the traditional fibers could be conveniently produced by electrospinning.

Electrospinning is a simple and versatile technique for generating a rich variety of nanofibers made of polymers, composites, and ceramics.[4] Recent efforts have made this technique a new platform for fabricating complex nanostructures having controllable hierarchical features. For example, a number of groups have demonstrated that electrospun nanofibers could be collected as single fibers, nonwoven mats, uniaxially aligned arrays, or multilayered films by modifying the electrospinning setup.[4,5] In addition to controlling macroscopic organization of nanofibers, electrospinning allows one to maneuver the secondary structures of individual fibers as well as to increase their structural complexity. To this end, nanofibers with core/sheath, hollow, or porous structures have been produced by using specially designed spinnerets or adjusting the spinning parameters.[6] Here we demonstrate that electrospinning and controlled calcination can be combined to provide a simple route to hierarchical nanostructures that are difficult to fabricate using other methods.

Our group and others have previously demonstrated that a variety of simple oxide nanofibers can be readily prepared

* To whom correspondence should be addressed. E-mail: xia@chem.washington.edu.
[†] Department of Chemistry, University of Washington.
[‡] The Molecular Foundry, Lawrence Berkeley National Laboratory.

10.1021/nl060928a CCC: $33.50
Published on Web 05/24/2006

by electrospinning a polymer solution containing the sol−gel precursors, followed by calcination at elevated temperatures.[7] Nanofibers consisting of mixed or complex oxides can be conveniently prepared by spinning a solution containing a mixture of precursors.[8] In particular, we observed that phase separation that often occurs in mixed oxides appeared to be essentially eliminated in an electrospinning process due to rapid evaporation of solvent from the thin jet.[8a] The properties (e.g., mechanical strength or catalytic activity) of ceramic materials are strongly dependent on the phase structure. In electrospun nanofibers of mixed oxides, ceramic phases are confined within a one-dimensional nanoscale volume. It would be of significance to study the evolution of each phase upon calcination in such a unique nanosystem.

Vanadium pentoxide (V_2O_5) and its mixtures with other oxides, particularly with titania (TiO_2), are important catalysts for some oxidation reactions, for example, reduction of NO_x with NH_3[9a] and the selective oxidation and reduction of hydrocarbons.[9b] They are also promising candidates for gas sensing[9c,d] and reversible intercalation in lithium batteries.[9e,f] By modifying the setup, we have successfully fabricated uniform nanofibers of V_2O_5/TiO_2 by electrospinning a 2-propanol solution containing poly(vinylpyrrolidone) (PVP), acetic acid, and two sol−gel precursors, titanium tetraisoproxide, $Ti(OiPr)_4$ and vanadium oxytriisopropoxide, $VO(OiPr)_3$, followed by calcination in air at elevated temperatures. Differing from our previous setup,[7a] we designed a solvent vapor jacket that covered the spinneret during electrospinning (Figure S1), preventing blockage of the nozzle caused by the rapid hydrolysis of $VO(OiPr)_3$. The mechanism is similar to that of two-capillary setup demonstrated by Larsen and co-workers.[10] The compositions of the fibers were controlled by varying the ratio of the two alkoxides in the feeding solution. In addition, it was found that the addition of a small amount of a surfactant, hexadecyltrimethylammonium bromide (HTAB), to the solution could help stabilize the spinning jet, improving the size uniformity of the resulting fibers.

In a typical procedure for electrospinning, 0.1 mL of glacial acetic acid and 0.2 mL of precursor solution—a mixture of 0.1 mL of $Ti(OiPr)_4$ and 0.1 mL of $VO(OiPr)_3$—were added in a glovebox to a solution containing 40 mg of PVP ($M_w \approx 1\,300\,000$), 10 mg of HTAB, and 0.7 mL of 2-propanol and the solution was vigorously mixed with the help of a VX-100 vortex mixer (Labnet, Edison, NJ). All chemicals were obtained from Aldrich. The solution was fed by a syringe pump (KDS-200, Stoelting, Wood Dale, IL) at a rate of 0.25 mL/h. The metallic needle was connected to a high-voltage power supply (ES30P-5W, Gamma High Voltage Research, Ormond Beach, FL), and a piece of aluminum foil or silicon wafer (Silicon Sense, Nashua, NH) was placed 7.5 cm below the tip of the needle to collect the nanofibers. The syringe needle was either a stainless steel needle or a disposable needle of gauge 26. The voltage was varied between 7.5 and 10.0 kV. The as-spun nanofibers were left in air for ~2 h to allow the hydrolysis of the alkoxides to go to completion (the moisture in air could also lead to the hydrolysis during the spinning process). The samples were then calcined at temperatures ranging from 375 to 575 °C for different periods of time in air.

Scanning electron microscopy (SEM) images were taken using a field-emission microscope (Sirion, FEI, Hillsboro, OR) operated at an accelerating voltage of 5 kV. Energy dispersive X-ray measurements were conducted using the EDAX system attached to the same microscope. High-resolution transmission electron microscopy (HRTEM) images and electron diffraction patterns were taken on a Tecnai G2 LaB6 high-resolution transmission electron microscope operated at 200 kV. X-ray diffraction (XRD) diffraction patterns were recorded on a Philips PW-1710 diffractometer (Cu Kα radiation).

Like other oxide fibers prepared by electrospinning,[7a,8a] the surface of as-spun or briefly calcined V_2O_5/TiO_2 nanofibers was very smooth (Figure 1A). As the calcination proceeded, however, new features started to evolve on the surface. The resulting morphology was dependent on the composition of the fibers and calcination conditions. Figure 1 shows the evolution of V_2O_5/TiO_2 nanofibers with a molar ratio of 1:1 (V:Ti) and calcined at 475 °C in air. After the as-spun fibers had been calcined for 10 min, the surface of the fibers became rough and short nanorods with a smooth surface appeared on the fibers. The nanorods were essentially perpendicular to the long axis of each fiber. The surface of the parent nanofibers became rougher and the number of nanorods increased as the calcination was prolonged. The growth of nanorods was fast at the beginning of calcination, slowed after about 1 h, and finally stopped after several hours. The typical length of the nanorods obtained after 1 h at 475 °C was 100−150 nm, and their nearly rectangular cross section was about 15 nm by 25 nm.

XRD analysis revealed that the as-spun fibers were amorphous, and the product calcined at 475 °C or above was composed of V_2O_5 in the shcherbinaite phase and TiO_2 mainly in the rutile phase (Figure S2). Energy dispersive spectroscopy (EDS) microanalysis on selected areas showed a V to Ti molar ratio of 10:1 in the nanorods and 1:1.05 in the fibers (Figure 2A), indicating that the nanorods were mainly made of V_2O_5 and the parent nanofibers were still a mixture of TiO_2 and V_2O_5. This conclusion was confirmed by the fact that an aqueous H_2O_2 solution could selectively dissolve the nanorods within seconds, leaving behind porous TiO_2 fibers (Figure S3).

The microstructure of the nanorods grown on the nanofibers was further investigated by HRTEM imaging. Panels B−D of Figure 2 show typical HRTEM images. Figure 2C shows lattice fringes of a nanorod with regular spacing of 0.58 nm, which is consistent with the interplanar distance of (200) planes of V_2O_5. We have also observed some nanorods with lattice fringes of 0.40 nm, which corresponds to the interplanar spacing of (101) planes. The well-resolved fringes confirm the single crystallinity of the V_2O_5 nanorods. The insets in Figure 2B show nanoprobe electron diffraction patterns from selected areas. The diffraction spots of the nanorods could be indexed to the (200) family of orthorhombic V_2O_5 crystals. These observations indicate that the single-crystal V_2O_5 nanorods were grown along the ⟨001⟩

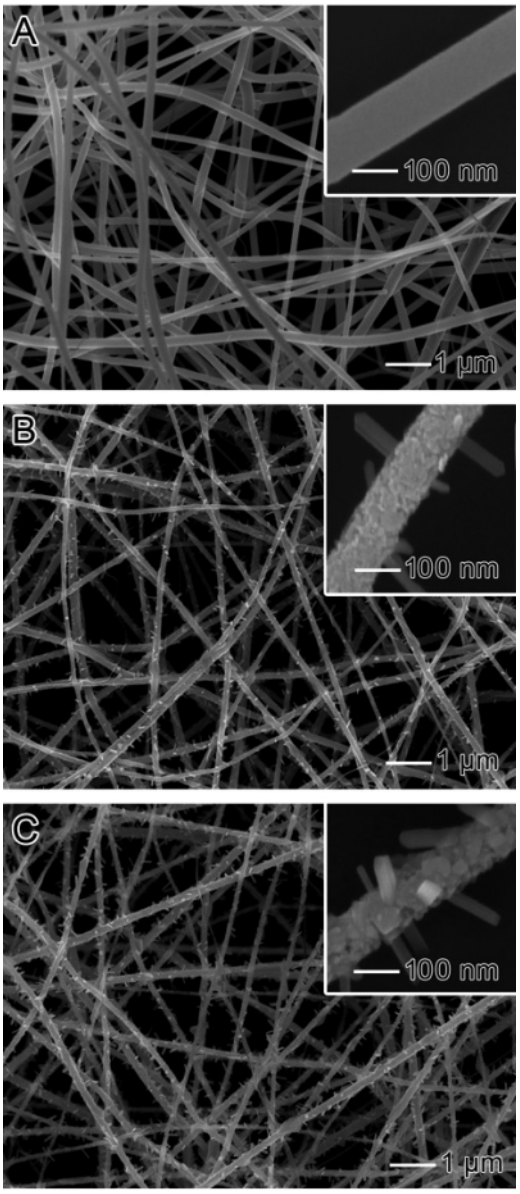

Figure 1. SEM images of $V_2O_5-TiO_2$ nanofibers that were electrospun from a 2-propanol solution containing 20% (wt/vol) $VO(OiPr)_3$, 20% $Ti(OiPr)_4$, 4% PVP, and 1% HTAB, followed by calcination at 475 °C for different periods of time: (A) 2.5 min; (B) 10 min; and (C) 60 min. Note that the ratio of $VO(OiPr)_3$ to $Ti(OiPr)_4$ (r) was 1:1.

direction. Electron diffraction from the parent nanofibers gave a ring pattern, indicative of the polycrystalline structure. All the diffractions could be indexed to those of V_2O_5 and the rutile phase of TiO_2. Close inspection at the junction of nanorods and nanofibers showed that the single-crystal V_2O_5 nanorods had their roots inside the polycrystalline V_2O_5/TiO_2 nanofibers (Figure 2D), suggesting that the V_2O_5 nanorods were not just loosely attached to the nanofiber surface.

We also varied the ratio of V_2O_5 to TiO_2 in the nanofibers and the calcination conditions to understand the formation mechanism of nanorod-on-nanofiber structures. First we studied the morphological evolution of pure V_2O_5 fibers upon calcination. Figure S4 shows SEM images of electrospun V_2O_5 fibers that had been calcined at 525 °C for different periods of time. After calcination for 5 min, the fibers displayed a rough surface due to the removal of PVP and the crystallization of V_2O_5. The fibers appeared to be an agglomeration of small particles with irregular shapes. As calcination proceeded, these particles evolved into bigger ones (t = 35 min) and then deformed to small, faceted crystals of several hundred nanometers in size (t = 70 min). Further calcination led to the formation of microrods up to tens of micrometers (t = 95 min). The crystallization of V_2O_5 is also dependent on the temperature for calcination. If the as-spun fibers were calcined at 475 °C or below, the fibers only exhibited a rough surface (Figure 3A) and no rodlike crystals with well-defined facets were observed.

The growth behavior of V_2O_5 crystals was changed once V_2O_5 was mixed with TiO_2 or other oxides. In the as-spun fibers, both V_2O_5 and TiO_2 were essentially amorphous and they were well mixed in the fibers. Upon calcination at elevated temperatures, both V_2O_5 and TiO_2 tended to crystallize, leading to significant phase separation and formation of new morphologies. The crystallization process of each compound could be very different from that of their pure systems. In our experiments, only the anatase phase was formed when V_2O_5-free TiO_2 fibers were calcined at 525 °C even for several hours. However, when mixed with V_2O_5, the main phase of titania in the fibers was rutile after calcination under the same condition (Figure S2). The result is consistent with previous reports that doping titania with a few percent of vanadia could significantly promote the phase transformation of anatase to rutile.[11] In addition to the difference in crystalline phase, the fibers of mixed oxides showed a rougher surface compared to pure titania nanofibers due to the bigger crystallites of rutile in the V_2O_5-doped fibers.

Mixing with titania did not make detectable changes to the crystal structure of V_2O_5. However, the existence of the titania phase in the fibers had a considerable effect on the size and shape of V_2O_5 crystals. Depending on the content of titania, the products exhibited different morphologies. As shown in panels A and B of Figure 3, no nanorod branches were observed when pure V_2O_5 fibers were calcined at 475 °C while some bumps appeared on the fibers containing titania with the ratio of V to Ti being 4:1. The bumps were shorter but wider than the nanorods grown on fibers when the number of moles was the same for V and Ti (Figure 1). No nanorods were observed if the ratio of V to Ti was less than 1:4.

In addition to the composition, the calcination temperature was another important parameter that affected the size and morphology of the V_2O_5 nanorods. Lower temperatures appeared to be favorable to the formation of thinner and more uniform nanorods. Panels C and D of Figure 3 show SEM images of the fibers calcined at 425 and 525 °C, respectively. The nanorods grew faster at 525 °C and they were shorter and thicker and the size distribution was less uniform than those obtained at 475 °C. At 425 °C, more uniform nanorods with a diameter of about 10 nm and a length up to 175−200 nm could be obtained after calcination for 6 h. Note that the ratio of V to Ti is 1:1, the same as those shown in Figures 1 and 2.

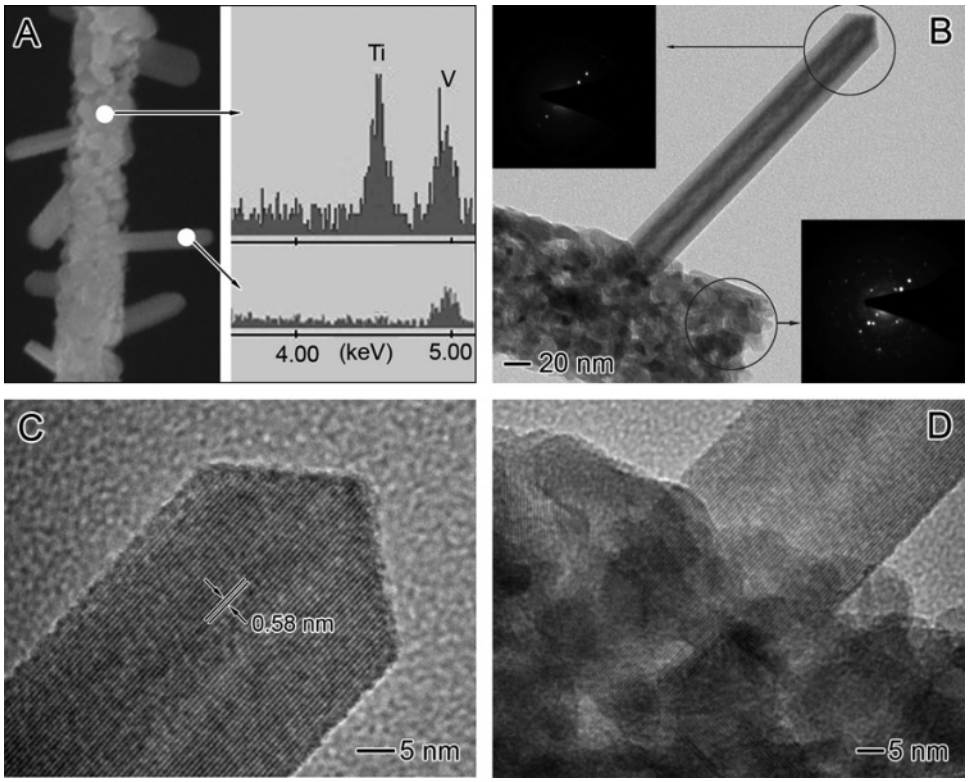

Figure 2. Structural analysis of the $V_2O_5-TiO_2$ nanofibers that were calcined at 475 °C for 30 min: (A) EDS microanalysis on selected areas; (B−C) HRTEM images and electron diffraction patterns of selected areas. The spinning solution was the same as in Figure 1.

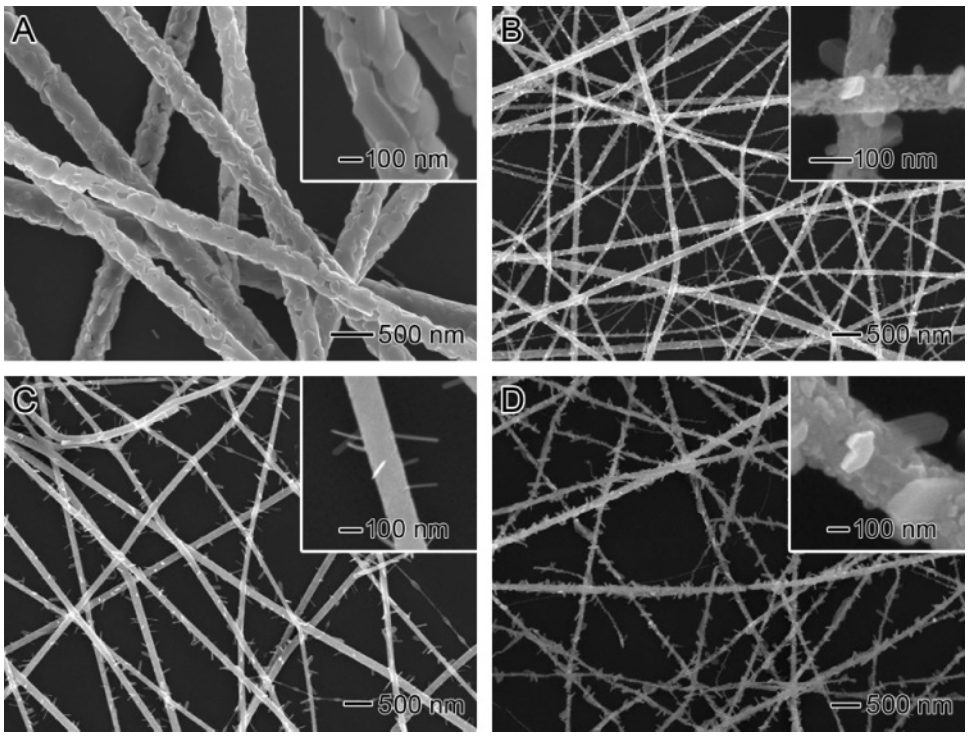

Figure 3. Typical SEM images of $V_2O_5-TiO_2$ nanofibers that were prepared by electrospinning from a 2-propanol solution containing different ratios (r) of $VO(OiPr)_3$ to $Ti(OiPr)_4$ and then calcining at various temperatures (T): (A) $r = 1{:}0$; $T = 475$ °C; (B) $r = 4{:}1$; $T = 475$ °C; (C) $r = 1{:}1$; $T = 425$ °C; and (D) $r = 1{:}1$; $T = 525$ °C.

These results clearly indicate that the shape and size of V_2O_5 nanorods could be controlled by the content of titania and calcination conditions. At the nucleation stage of V_2O_5 nanorods, the presence of titania networks in the composite fibers or low temperature favored the formation of small nuclei, leading to the formation of thin and long nanorods. The spatial confinement of vanadia by titania might also force some of the V_2O_5 nanocrystals to grow towards the outside

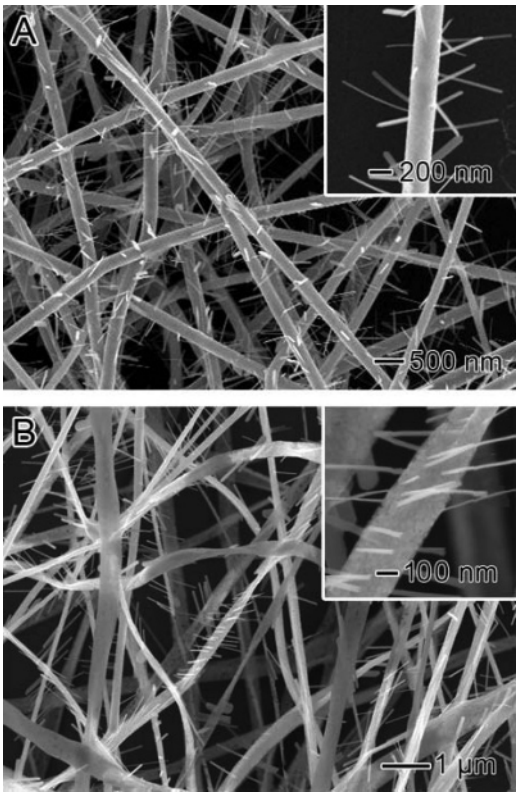

Figure 4. (A) SEM images of $V_2O_5-TiO_2-Ta_2O_5$ nanofibers that were electrospun from a 2-propanol solution containing 40% (wt/vol) of $VO(OiPr)_3$ and $Ti(OiPr)_4$ (r = 1:1) with 3% $TaO(OiPr)_3$, 4% PVP, and 1% HTAB. The fibers were then calcined at 425 °C for 6 h. (B) SEM images of $V_2O_5-SiO_2$ nanofibers that were electrospun from a 2-propanol solution containing 40% (wt/vol) 1:3 mixture of $VO(OiPr)_3$ and $Si(OEt)_4$, 4% PVP, and 1% HTAB. The fibers were calcined at 575 °C for 20 min.

of the fibers to generate nanorods on the fibers while some were trapped in the fibers. Furthermore, the presence of titania might influence the crystallization and diffusion rates of V_2O_5 and further promote the growth of V_2O_5 nanorods.

Our experiments showed that the shape and size of V_2O_5 nanorods were also related to the crystal structure and size of titania nanoparticles in the composite fibers. It has been previously reported that the addition of Ta_2O_5 into titania could prevent the crystallization of titania and the phase transformation from anatase to rutile.[12] We found that the content of the anatase phase was significantly increased when a small amount of Ta_2O_5 was introduced into the V_2O_5/TiO_2 fibers and the resulting fibers showed smoother surfaces than Ta_2O_5-free ones (Figure 4A), implying the crystalline size of titania nanoparticles in these fibers could be smaller. The V_2O_5 nanorods grown on the Ta_2O_5-incorporated fibers were thinner and considerably longer. The titania network consisting of smaller-sized nanoparticles might be able to provide a higher level of confinement to the nucleation and growth of V_2O_5 nanorods. Ta_2O_5 itself could also affect the crystallization of V_2O_5 nanorods.

In addition to TiO_2, our preliminary experiments showed that other oxides such as SiO_2 could serve as the suitable matrix for generating the nanorod-on-nanofiber structure. Depending on the composition, the resulting hierarchical structures could be further tuned. Figure 4B shows SEM images of a sample of SiO_2/V_2O_5 fibers that was electrospun from a solution containing tetraethyl orthosilicate, $Si(OEt)_4$, and $VO(OiPr)_3$ and were then calcined at 575 °C for 20 min. In this sample, the distribution of V_2O_5 in the fibers was not uniform, possibly due to the big difference in the hydrolysis rate of the two alkoxide precursors. This result suggests that the distribution of V_2O_5 nanorods on the fibers could be controlled by adjusting the composition and phase separation of the parent fibers and a new hierarchical structure was also achieved.

In summary, we have demonstrated that single-crystal V_2O_5 nanorods could directly grow on electrospun V_2O_5/TiO_2 composite nanofibers during calcination. The size of the resulting nanorods could be controlled by the composition of the fibers and the calcination temperature. This work provides a simple route to the nanorod-on-nanofiber hierarchical structure. More generally, this work suggests that postspinning treatment of electrospun nanofibers of mixed oxides offers an additional means to fine tune the phase structure and morphology of nanofibers, enabling the fabrication of complex architectures. Mixed oxides are widely used in many technologically important fields such as catalysis, chemical sensing, and rechargeable batteries. To achieve optimal performances, hierarchical structures with controlled crystalline structures and spatial distribution of each component are often desired.[13] Electrospinning allows convenient fabrication of hierarchically structured oxide materials with high porosity, surface area, as well as controlled compositions and sizes. In particular, electrospun nanofibers are small in diameter but long in length, which makes it very convenient to study both their microstructure (as shown in this work) and their macroscopic properties. All these features make electrospun nanofibers an ideal platform for studying the structure−property relationship, which will be beneficial to the design of high-performance materials such as catalysts and electrodes for batteries.

Acknowledgment. This work was supported in part by an AFOSR-MURI grant on smart skin materials awarded to the University of Washington, and a research fellowship from the David and Lucile Packard Foundation. Y.X. is a Camille Dreyfus Teacher Scholar (2002) and an Alfred P. Sloan Research Fellow (2000). This work was performed in part at the Nanotech User Facility (NTUF) at the University of Washington, a member of the National Nanotechnology Infrastructure Network (NNIN) funded by the NSF. R.O. thanks the Ecole Normale Supérieure, Paris, for a scholarship. D.L. is an INEST Postdoctoral Fellow supported by Phillip Morris USA. Y.Y. is supported by the Director, Office of Energy Research, Office of Science, Division of Materials Sciences, of the U.S. Department of Energy under contract no. DE-AC02-05CH11231.

Supporting Information Available: Figures showing a schematic of the electrospinning spinneret, XRD diffraction pattern taken from electrospun nanofibers, and SEM images of $V_2O_5-TiO_2$ nanofibers. This material is available free of charge via the Internet at http://pubs.acs.org.

References

(1) See a few examples: (a) Lauhon, L. J.; Gudiksen, M. S.; Wang, D.; Lieber, C. M. *Nature* **2002**, *420*, 57. (b) Milliron, D. J.; Hughes, S. M.; Cui, Y.; Manna, L.; Li, J.; Wang, L.-W.; Alivisatos, A. P. *Nature* **2004**, *430*, 190. (c) Jun, Y.-W.; Lee, S.-M.; Kang, N.-J.; Cheon, J. *J. Am. Chem. Soc.* **2001**, *123*, 5150. (d) Lao, J. Y.; Wen, J. G.; Ren, Z. F. *Nano Lett.* **2002**, *11*, 1287. (e) Wang, Z. L.; Pan, Z. W. *Adv. Mater.* **2002**, *14*, 1029. (f) Gao, P.; Wang, Z. L. *J. Phys. Chem. B* **2002**, *106*, 12653. (g) Wan, Q.; Wei, M.; Zhi, D.; MacManus-Driscoll, J. L.; Blamire, M. G. *Adv. Mater.* **2006**, *18*, 234. (h) Dick, K. A.; Deppert, K.; Larsson, M. W.; Martensson, T.; Seifert, W.; Wallenberg, L. R.; Samuelson, L. *Nat. Mater.* **2004**, *3*, 380. (i) Zhang, D.-F.; Sun, L.-D.; Jia, C.-J.; Yan, Z.-G.; You, L.-P.; Yan, C.-H. *J. Am. Chem. Soc.* **2005**, *127*, 13492.

(2) Li, D.; McCann, J. T.; Gratt, M.; Xia, Y. *Chem. Phys. Lett.* **2004**, *394*, 387.

(3) Hou, H.; Reneker, D. H. *Adv. Mater.* **2004**, *16*, 69.

(4) (a) Li, D.; Xia, Y. *Adv. Mater.* **2004**, *16*, 1151. (b) Reneker, D. H.; Chun, I. *Nanotechnology* **1996**, *7*, 216.

(5) (a) Li, D.; Wang, Y.; Xia, Y. *Nano Lett.* **2003**, *3*, 1167. (b) Li, D.; Wang, Y.; Xia, Y. *Adv. Mater.* **2004**, *16*, 361. (c) Li, D.; Ouyang, G.; McCann, J. T.; Xia, Y. *Nano Lett.* **2005**, *5*, 913. (d) Theron, A.; Zussman, E.; Yarin, A. L. *Nanotechnology* **2001**, *12*, 384. (e) Zussman, E.; Theron, A.; Yarin, A. L. *Appl. Phys. Lett.* **2003**, *82*, 973. (f) Xu, C. Y.; Inai, R.; Kotaki, M.; Ramakrishna, S. *Biomaterials* **2004**, *25*, 877.

(6) (a) Li, D.; Xia, Y. *Nano Lett.* **2004**, *4*, 933. (b) Loscertales, I. G.; Barrero, A.; Marquez, M.; Spretz, R.; Velarde-Ortiz, R.; Larsen, G. *J. Am. Chem. Soc.* **2004**, *126*, 5376. (c) Sun, Z.; Zussman, E.; Yarin, A. L.; Wendorff, J. H.; Greiner, A. *Adv. Mater.* **2003**, *15*, 1929. (d) Yu, J.; Fridrikh, S. V.; Rutledge, G. C. *Adv. Mater.* **2004**, *16*, 1562. (e) Li, D.; McCann, J. T.; Xia, Y. *Small* **2005**, *1*, 83. (f) Lin, T.; Wang, H.; Wang, X. *Adv. Mater.* **2005**, *17*, 2699. (f) Zhang, Y. Z.; Huang, Z. M.; Xu, X. J.; Lim, C. T.; Ramakrishna, S. *Chem. Mater.* **2004**, *16*, 3406. (g) Kidoaki, S.; Kwon, I. K.; Matsuda, T. *Biomaterials* **2005**, *26*, 37.

(7) (a) Li, D.; Xia, Y. *Nano Lett.* **2003**, *3*, 555. (b) Larsen, G.; Velarde-Ortiz, R.; Minchow, K.; Barrero, A.; Loscertales, I. G. *J. Am. Chem. Soc.* **2003**, *125*, 1154. (c) Viswanathamurthi, P.; Bhattarai, N.; Kim, H. Y.; Lee, D. R.; Kim, S. R.; Morris, M. A. *Chem. Phys. Lett.* **2003**, *374*, 79. (d) Wang, Y.; Furlan, R.; Ramos, I.; Santigano-Aviles, J. I. *Appl. Phys. A* **2004**, *78*, 1043. (e) Madhugiri, S.; Zhou, W.; Ferraris, J. P.; Balkus, K. J., Jr. *Microporous Mesoporous Mater.* **2003**, *63*, 75. (f) Li, D.; McCann, J. T.; Marquez, M.; Xia, Y. *J. Am. Ceram. Soc.*, in press.

(8) (a) Li, D.; Herricks, T.; Xia, Y. *Appl. Phys. Lett.* **2003**, *83*, 4586. (b) Dai, H.; Gong, J.; Kim, H.; Lee, D. *Nanotechnology* **2002**, *13*, 674.

(9) (a) Hoang-Van, C.; Zegaoui, O.; Pichat, P. *J. Non-Cryst. Solids* **1998**, *225*, 157. (b) Centi, G. *Appl. Catal., A* **1996**, *147*, 267. (c) Biette, L.; Carn, F.; Maugey, M.; Achard, M. F.; Maquet, T.; Steunou, N.; Livage, T.; Serier, H.; Backov, R. *Adv. Mater.* **2005**, *17*, 2970. (d) Carotta, M. C.; Ferroni, M.; Gherardi, S.; Guidi, V.; Malagu, C.; Martinelli, G.; Sacerdoti, M.; Di Vona, M. L.; Licoccia, S.; Traversa, E. *J. Eur. Ceram. Soc.* **2004**, *24*, 1409. (e) Sides, C. R.; Martin, C. R. *Adv. Mater.* **2005**, *17*, 125. (f) Lee, K.; Cao, G. *J. Phys. Chem. B* **2005**, *109*, 11880.

(10) Larsen, G.; Spretz, R.; Velarde-Ortiz, R. *Adv. Mater.* **2004**, *16*, 166.

(11) Oliveri, G.; Ramis, G.; Busca, G.; Escribano, V. S. *J. Mater. Chem.* **1993**, *3*, 1239.

(12) Sacerdoti, M.; Dalconi, M. C.; Carotta, M. C.; Cavicchi, B.; Ferroni, M.; Colonna, S.; Di Vona, M. L. *J. Solid State Chem.* **2004**, *177*, 1781.

(13) Stelzer, J. B.; Fait, M.; Bentrup, U.; Kubias, B.; Eberle, H.-J.; Caro, J. *Chem. Eng. Technol.* **2004**, *27*, 1296.

NL060928A